

# Synthesis of Uniform Zinc Peroxide Nanoparticles for Antibacterial Application

YING XIONG, SONG SHEN<sup>1</sup> AND Z. YI\*

Department of Pharmacy, Affiliated Hospital of Nantong University, Yancheng Third People's Hospital, Yancheng, Jiangsu 224500, <sup>1</sup>Jiangsu University, Zhenjiang, Jiangsu 212013, China

## Xiong *et al.*: Role of Zinc Peroxide in Antibacterial Activity

Peroxides and metals have been emerged as alternative antibacterial agents. However, the application of peroxides or metals alone for antibacterial treatment cannot yield satisfactory results. Combined therapy based on peroxides and metals is expected to generate synergistic effects. In this work, uniform zinc peroxide nanoparticles with an average size of 60 nm were synthesized as antimicrobial agent. Zinc peroxide nanoparticles were relatively stable in a neutral environment and showed quick release of hydrogen peroxide and zinc ion in acidic environment. After incubation with *Escherichia coli* and *Staphylococcus aureus*, large amount of reactive oxygen species was generated. Zinc peroxide nanoparticles illustrated outstanding antibacterial activity for *Escherichia coli* and *Staphylococcus aureus*, holding a great potential to be a highly efficient antibacterial agent.

**Key words:** Metal peroxides, antibacterial, reactive oxygen species, zinc peroxide, nanoparticles, *Escherichia coli* and *Staphylococcus aureus*

Treatment of bacterial infection is still a challenge due to the emergence of bacterial resistance, which leads to the exploration of alternative antibacterial and treatments<sup>[1,2]</sup>. Therefore, it is extremely urgent to synthesize novel materials with broad-spectrum antimicrobial activity to enhance or replace traditional antibiotics. These drugs play crucial role in surgeries, immunotherapy, and other medical procedures, significantly reducing human mortality and morbidity rates<sup>[3]</sup>. The mechanism of antibiotic resistance is complex and bacteria generally reduce the effectiveness of antibiotics through several different mechanisms<sup>[4]</sup>. These include reducing their permeability<sup>[5]</sup>, actively pumping antibiotics out of the cell<sup>[6]</sup>, altering or modifying the antibiotic's target affinity<sup>[7]</sup>, rendering the antibiotic inactive, or modifying it in some way<sup>[8,9]</sup>.

Peroxides and metals hold great promise as alternatives to antibiotics. Peroxides, such as Hydrogen peroxide (H<sub>2</sub>O<sub>2</sub>) and Sodium hypochlorite (NaClO), can cause oxidation of bacteria and has been widely used as bactericide<sup>[10,11]</sup>. These compounds generate Reactive Oxygen Species

(ROS), which can disrupt essential cellular functions and damage bacterial cells by oxidizing cellular components<sup>[12,13]</sup>. Metals kill bacteria by different mechanisms; when metals come in contact with bacterial cells, they disrupt the outer membranes and penetrate the cells. Inside the cells, these metal ions interfere with various cellular processes, such as depleting antioxidants, disrupting the normal functioning of proteins and enzymes, damaging the cellular membranes and interfering with the electron transport, thereby causing genotoxicity<sup>[14,15]</sup>. Considering different antibacterial mechanisms, it is reasonable to deduce that the combination of the peroxides and metals is a potential method to enhance the antimicrobial activity. Among different metal oxides, Zinc Oxide (ZnO) is a widely used antimicrobial and/or antifungal agent due to its advantages such as lower cytotoxicity, better selectivity and higher stability<sup>[16,17]</sup>. Previous studies have shown that Zinc peroxide (ZnO<sub>2</sub>) Nanoparticles (NPs) can release Oxygen (O<sub>2</sub>) triggered by temperature or pH in dispersing media<sup>[18]</sup>. It can be proved that the nanoparticles continuously release O<sub>2</sub> for about 3 d at a pH<7.5 in an aqueous dispersion. The amount

---

\*Address for correspondence  
E-mail: j598shensong@163.com

of  $O_2$  released depends on the different samples and is controlled by the different compositions and selected pH values of the samples.

In this work, we synthesized uniform  $ZnO_2$  NPs to further improve the antimicrobial activity (fig. 1).  $ZnO_2$  NPs were synthesized by oxidizing zinc acetate with  $H_2O_2$  using Polyvinylpyrrolidone (PVP) as stabilizer<sup>[19]</sup>. We evaluated the reaction of  $ZnO_2$  NPs in Phosphate Buffered Saline (PBS) at pH 5.5 and 7.4 and demonstrated that the Zinc ( $Zn^{2+}$ ) ions and hydrogen peroxide release rates are greatly accelerated in acidic environments. Simultaneously, we found that in the presence of  $ZnO_2$  NPs, ROS can be produced in both *Escherichia coli* (*E. coli*) and *Staphylococcus aureus* (*S. aureus*), laying the foundation for the antibacterial effect of  $ZnO_2$  NPs. The toxicity experiments were conducted to explore the antibacterial effect of  $ZnO_2$  NPs, which opened up a new path for the future application of  $ZnO_2$ .

## MATERIALS AND METHODS

We used Transmission Electron Microscopy (TEM) for characterization of the obtained  $ZnO_2$  NPs. As shown in fig. 2a, the  $ZnO_2$  NPs were uniform in spherical morphology with an average diameter of 60 nm; Dynamic Light Scattering (DLS) was used to determine the hydrated particle size by. The average size increased to 70 nm due to the inclusion of solvation shell (fig. 2b). X-Ray Diffraction (XRD) was utilized to detect the crystal structure of the  $ZnO_2$  NPs. As shown in fig. 3a, the pattern of  $ZnO_2$  with typical peaks at  $31^\circ$ ,  $37^\circ$ ,  $53^\circ$  and  $63^\circ$  which was supported by the Joint Committee on Powder Diffraction Standards (JCPDS) (having number: 00-076-1364), attributing to cubic zinc blende structure<sup>[20,21]</sup>. We have noticed that the diffraction peaks of  $ZnO_2$  NPs were wide and weak, indicating relatively small size of the nanocrystals. Small sized crystals implied the capability of PVP in inhibiting the formation and growth of crystals.

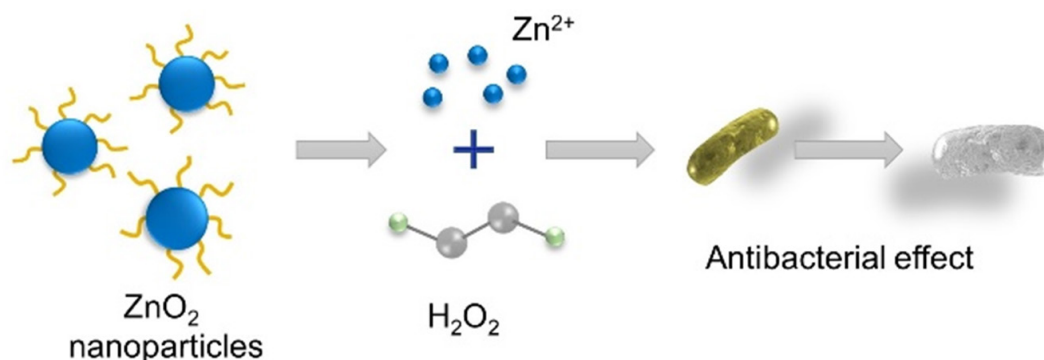


**Fig. 1:** Schematic diagram showing the dissolution of  $ZnO_2$  nanoparticles and the formation of  $Zn^{2+}$  and  $H_2O_2$  in acidic environment  
Note:  $Zn^{2+}$  and  $H_2O_2$  effectively damage the bacteria

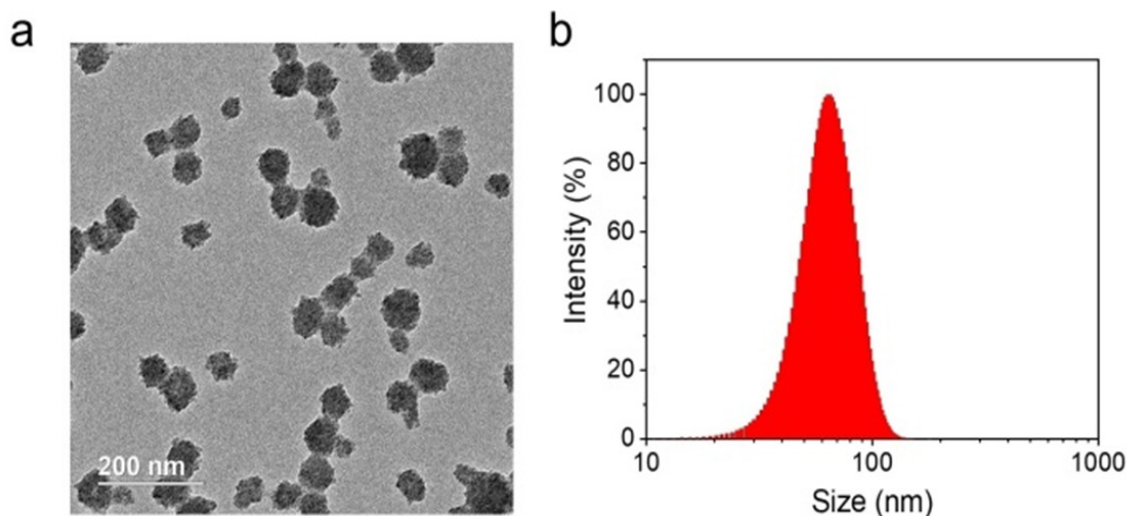


**Fig. 2:**  $ZnO_2$  NPs measured by dynamic light scattering, (a): TEM image and (b): Hydrodynamic diameter

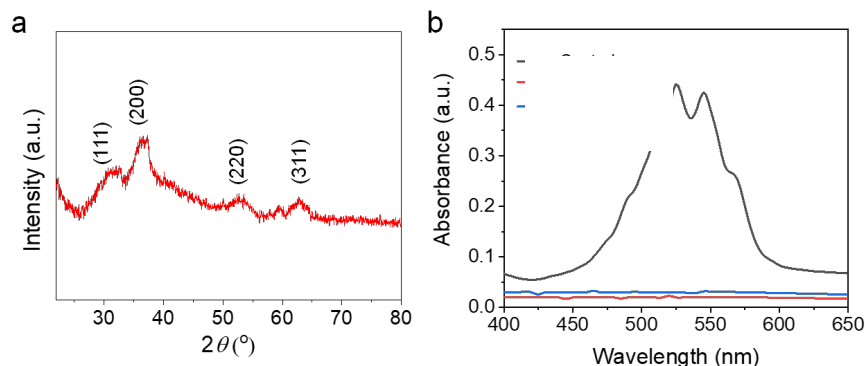


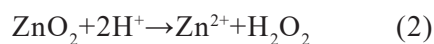
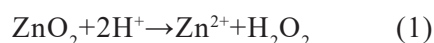
**Fig. 3: Typical peaks demonstrating the presence of peroxy groups in ZnO<sub>2</sub> NPs, (a): XRD patterns of the synthesized NPs and (b): Colorimetric analysis**

Note: (■): Control; (■): H<sub>2</sub>O<sub>2</sub> and (■): ZnO<sub>2</sub>

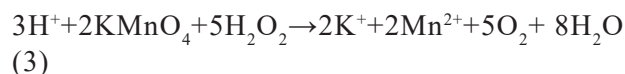
PVP molecules play an essential role in the formation of the nanocrystals during the formation of ZnO<sub>2</sub> NPs. PVP can chelate with metal ions and then assist the ions to form ZnO<sub>2</sub> nanocrystals in the presence of oxidants. From the TEM image of ZnO<sub>2</sub> NPs, we found that the ZnO<sub>2</sub> NPs were composed of many small nanocrystals. The formation of the larger nanocrystals aggregations was because of the tendency to reduce the high surface energy. Meanwhile, PVP can also prevent the sudden and random aggregation of the nanocrystals to help the formation of uniform ZnO<sub>2</sub> NPs owing to the steric hindrance effect of the PVP.

## RESULTS AND DISCUSSION

In neutral and acidic environment, ZnO<sub>2</sub> NPs could react with Water (H<sub>2</sub>O) and Hydrogen ions (H<sup>+</sup>) to produce H<sub>2</sub>O<sub>2</sub> by the reactions (1) and (2), respectively.



In acidic environment, ZnO<sub>2</sub> NPs reacted with H<sup>+</sup> to generate H<sub>2</sub>O<sub>2</sub> as per reaction (1). Thus generated H<sub>2</sub>O<sub>2</sub> was determined by Potassium Permanganate (KMnO<sub>4</sub>)-based colorimetric method.



Purple colored Permanganate (MnO<sub>4</sub><sup>-</sup>) ion was reduced by peroxy groups to form colourless Manganese (Mn<sup>2+</sup>) ion. As shown in fig. 3b, the purple color of MnO<sub>4</sub><sup>-</sup> in acidic solution disappeared after addition of H<sub>2</sub>O<sub>2</sub> or ZnO<sub>2</sub> NPs, indicating the formation of H<sub>2</sub>O<sub>2</sub> in the acidic medium.

Most metal oxides are unstable and will hydrolyze in H<sub>2</sub>O. However, the hydrolysis rate is quite

different. Calcium peroxide (CaO<sub>2</sub>) NPs hydrolyze quickly in aqueous solution, while the hydrolysis of Copper peroxide (CuO<sub>2</sub>) was much slower<sup>[22,23]</sup>. We have evaluated the reaction of ZnO<sub>2</sub> NPs at pH 5.5 and 7.4 Phosphate Buffer Saline (PBS) and determined the release rates of Zn<sup>2+</sup> and H<sub>2</sub>O<sub>2</sub>. As shown in fig. 4a and fig. 4b, both Zn<sup>2+</sup> and H<sub>2</sub>O<sub>2</sub> were gradually released from the ZnO<sub>2</sub> NPs at pH 5.5, showing a cumulative release >60 % at 4 h. In contrast, the release rates were slower at pH 7.4 PBS that only 5 % was released after 6 h. These results indicate that the ZnO<sub>2</sub> NPs are relatively stable in neutral environment and will decompose quickly in acidic medium. The bacteria acidic microenvironment also facilitates the release of zinc and hydrogen peroxide.

It is reported that bacterial infection will form weak acidic microenvironment. Hence, H<sub>2</sub>O<sub>2</sub> is expected to generate after incubation of the bacteria with ZnO<sub>2</sub> NPs. The intracellular ROS was detected using 2,7-Dichloro-dihydro-Fluorescein Diacetate (DCFH-DA) as an indicator, which is non-fluorescent and can be oxidized by ROS to form fluorescent Dichlorodihydrofluorescein (DCF).

As shown in fig. 5a and fig. 5b, barely visible fluorescence was observed in *E. coli* and *S. aureus* without the treatment of ZnO<sub>2</sub> NPs. In contrast, bacteria treated with ZnO<sub>2</sub> NPs illustrated bright green fluorescence, indicating the generation of ROS in bacteria. We also noticed that the strength of the fluorescence was time dependent. The fluorescence intensities of *E. coli* and *S. aureus* at 2 h were 1.58 and 2.15 times to those of 0.5 h, respectively (fig. 6a and fig. 6b). It is necessary to search appropriate incubation time to enhance the antibacterial effects of ZnO<sub>2</sub> NPs. The generated ROS will cause oxidative stress to bacterial cells

and result in the damage to protein, membrane lipids and Deoxyribonucleic Acid (DNA).

In addition to the evaluation of size, morphology, crystallinity, generation of ROS and the O<sub>2</sub> release performance of ZnO<sub>2</sub> NPs were also studied. Previous studies have indicated that O<sub>2</sub> release from ZnO<sub>2</sub> NPs was related to temperature or pH values. We investigated its O<sub>2</sub> release in aqueous solutions with different pH values. ZnO<sub>2</sub> NPs dissociates into Zn<sup>2+</sup> ions and H<sub>2</sub>O<sub>2</sub> in acidic aqueous media, while H<sub>2</sub>O<sub>2</sub> can be catalyzed by the metal on the NPs surface to produce into H<sub>2</sub>O and O<sub>2</sub>. We measured the time-dependent release of O<sub>2</sub> from ZnO<sub>2</sub> NPs in different pH media using an O<sub>2</sub> meter.

The determinations were performed in degassed PBS in nitrogen atmosphere to influence of atmospheric O<sub>2</sub> on quantification. PBS solution without ZnO<sub>2</sub> nanoparticles determined in identical conditions was used as control. The experiment was performed at room temperature (T=25°) in neutral and weakly acidic PBS with pH values of 7.4 and 6.5, respectively. The results indicated that there is a constant O<sub>2</sub> release for at least 96 h and then reached a plateau resulting in a saturation curve. Since PBS solution was degassed and placed under a nitrogen atmosphere, there was negligible O<sub>2</sub> present during the determination. After dispersing the NPs in PBS, O<sub>2</sub> was constantly released, causing the increase of O<sub>2</sub> concentration in H<sub>2</sub>O. When the reaction of NPs with H<sub>2</sub>O was completed, O<sub>2</sub> concentration reached the plateau. Considering the high solubility of O<sub>2</sub> in H<sub>2</sub>O (8.7-8.4 mg/l at 25°)<sup>[24,25]</sup>, the plateau was because of the nanoparticle deactivation. The determinations of the ZnO<sub>2</sub> nanoparticles in different pH value i.e., at 6.5 revealed that the amount of released O<sub>2</sub> was dependent on the pH. As shown in fig. 7, the O<sub>2</sub> release increased as the decrease of pH value. The amount of released O<sub>2</sub> increased from 0.73 to 2.1 mg/l with changing pH value from 7.4 and 6.5. These results were in line with the expectations because the acidic environment accelerates the O<sub>2</sub> release by accelerating the decomposition of the ZnO<sub>2</sub> NPs.

ZnO is a transition metal oxide and semiconductor with wide band gap (3.3 eV). Oxidizing character and oxidizing sites would be created once there is radiation with energy larger than the band

gap of the ZnO. Thus, formed oxidizing sites are capable of oxidizing water molecules and hydroxide anions to form strong oxidizing species and generate antibacterial effect. For ZnO<sub>2</sub> NPs, can react with H<sub>2</sub>O and H<sup>+</sup> to release ROS and are expected to cause better antibacterial effect. The antibacterial activity of the ZnO<sub>2</sub> NPs was then evaluated using *E. coli* and *S. aureus* as model bacteria by colony counting assay method. To comprehensively understand the antibacterial efficiency, ZnO NPs were used as control. As presented in fig. 8a and fig. 8b, ZnO<sub>2</sub> NPs reduced the number of *E. coli* and *S. aureus* by about 40 % and 50 %, respectively. The toxicity of ZnO<sub>2</sub> NPs towards the *E. coli* and *S. aureus* was much stronger than the ZnO NPs. The increased toxicity of ZnO<sub>2</sub> NPs should be attributed to the synergistic effect of H<sub>2</sub>O<sub>2</sub> and Zn<sup>2+</sup>. The effect of ZnO<sub>2</sub> NPs was comparable to H<sub>2</sub>O<sub>2</sub>. Although ZnO NPs are considered as a bacteriostatic agent, their effect could be further improved by forming peroxides. For the antibacterial mechanism, it is reported that metal NPs will attach to the surfaces of bacteria by the adsorption and electrostatic interaction, resulting in damage to the cell membrane. Meanwhile, the released Zn<sup>2+</sup> ions can chelate with teicoic and lipoteichoic acids, and then be carried by passive diffusion across membrane proteins<sup>[16]</sup>.

The Minimum Inhibitory Concentration (MIC) values of the ZnO<sub>2</sub> NPs were further studied by micro-broth dilution method; MICs against *E. coli* and *S. aureus* were 90 and 60 µg/ml, respectively. In contrast, MICs of ZnO NPs for *E. coli* and *S. aureus* were 350 and 200 µg/l, respectively. These results were in agreement with the results obtained by colony counting assay method, suggesting the enhancement of the bacterial viability inhibition effect.

In summary, ZnO<sub>2</sub> NPs with uniform size were successfully synthesized with the help of PVP through a facile method. NPs could release H<sub>2</sub>O<sub>2</sub> and Zn<sup>2+</sup> quickly in acidic environment. ZnO<sub>2</sub> NPs showed outstanding antibacterial activity, owing to the synergistic effect of released H<sub>2</sub>O<sub>2</sub> and Zn<sup>2+</sup>. Although the ZnO<sub>2</sub> NPs were relatively stable in H<sub>2</sub>O, it is difficult to store for long-time storage in aqueous medium. For clinic application, dispersing the ZnO<sub>2</sub> NPs in non-aqueous media, such as glycerin, may be a feasible method to enhance the stability.

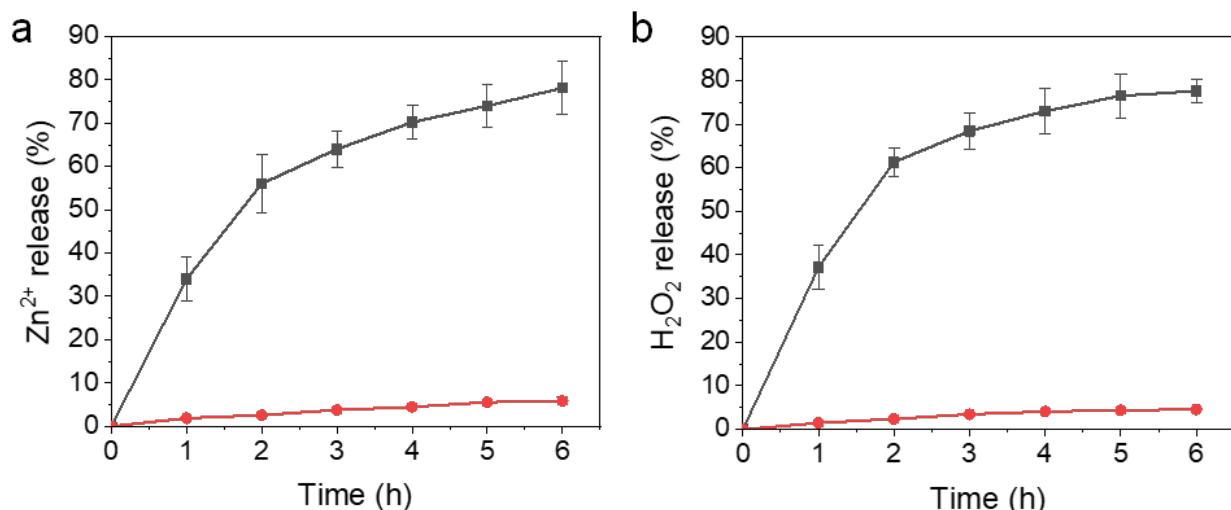


Fig. 4: Release profiles of Zn<sup>2+</sup> and H<sub>2</sub>O<sub>2</sub> from ZnO<sub>2</sub> NPs at a pH of 5.5 and 7.4 of PBS, (a): Zn<sup>2+</sup> and (b) H<sub>2</sub>O<sub>2</sub>  
 Note: (■): pH 5.5 and (●): pH 7.4

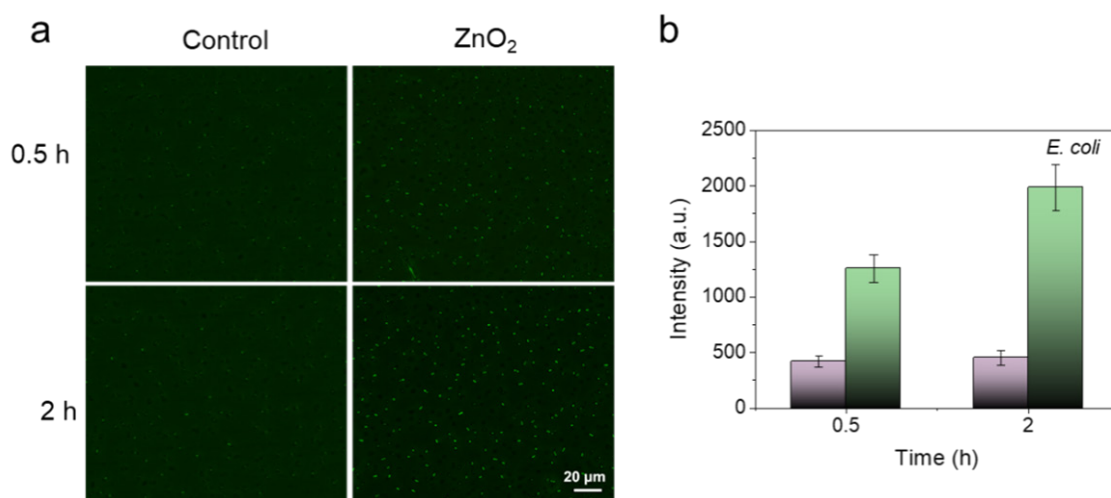


Fig. 5: Fluorescence intensity of *E. coli*, (a): DCFH-DA stained *E. coli* showing intracellular ROS after treated for 0.5 and 2 h and (b): Corresponding fluorescence intensity  
 Note: (■): Control and (■): ZnO<sub>2</sub>

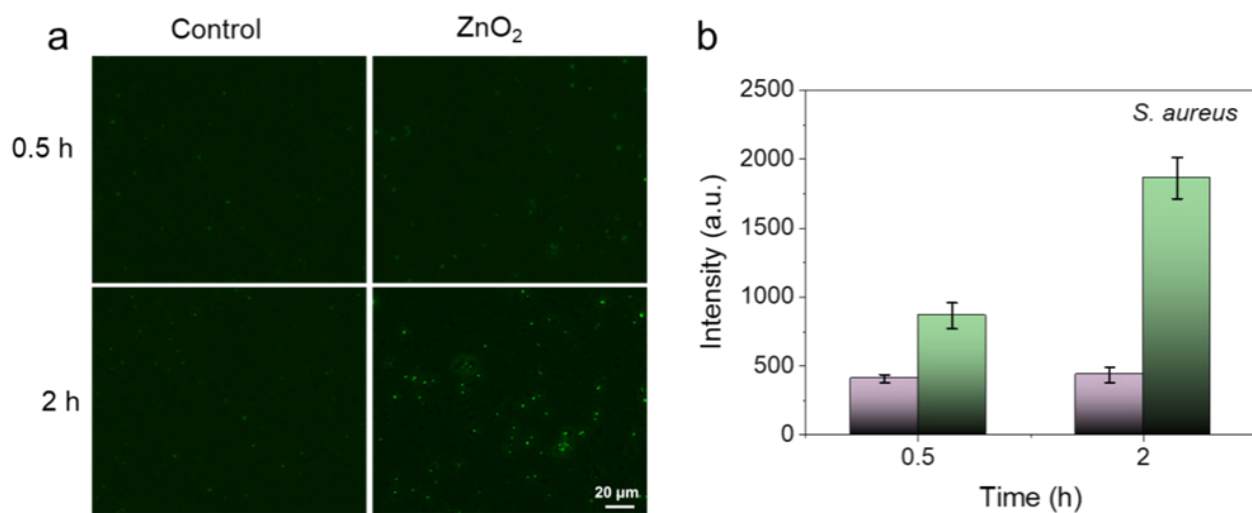


Fig. 6: Fluorescence intensity of *S. aureus*, (a): DCFH-DA stained *S. aureus* showing intracellular ROS after treated for 0.5 and 2 h and (b): Corresponding fluorescence intensity  
 Note: (■): Control and (■): ZnO<sub>2</sub>

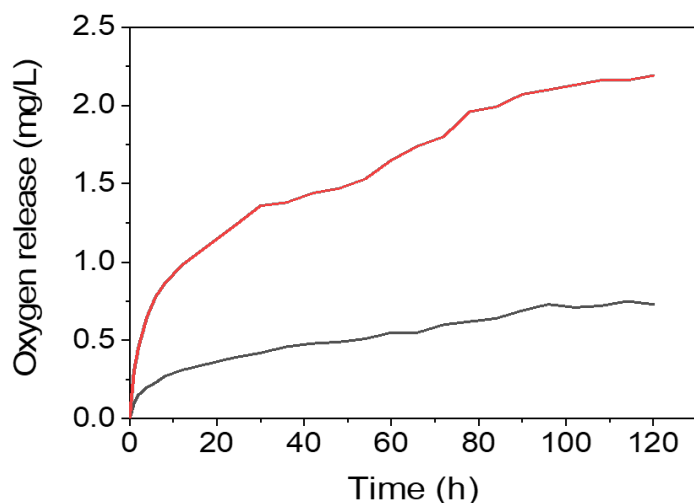


Fig. 7: Time dependent  $O_2$  release measurements in aqueous media at different pH values  
 Note: (■): pH 7.4 and (■): pH 6.5

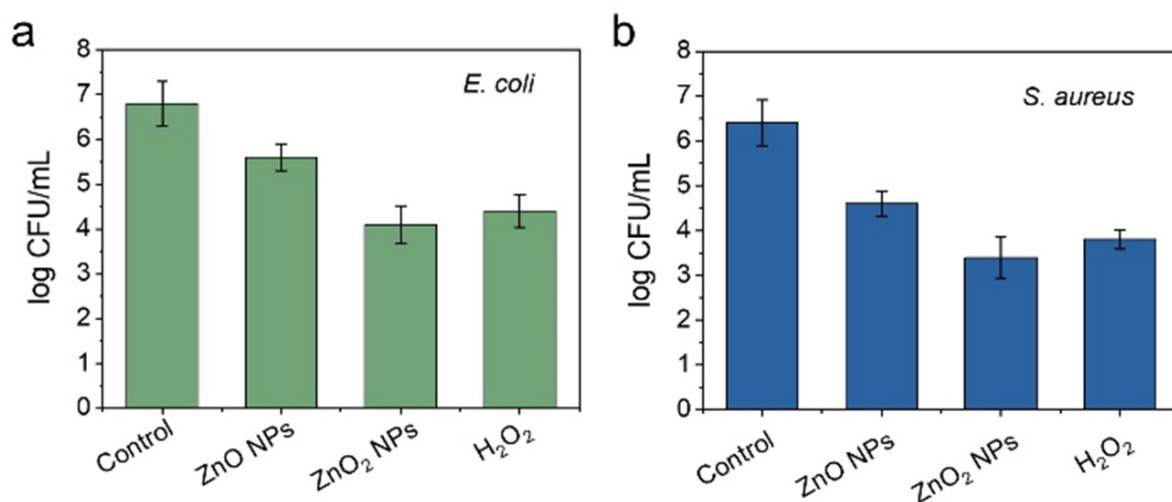


Fig. 8: Antibacterial effects of  $H_2O_2$ , ZnO NPs and ZnO<sub>2</sub> NPs by colony count assay (n=3), (a): *E. coli* and (b): *S. aureus*

#### Acknowledgement:

This study was financially supported by the National Natural Science Foundation of China. (Grant No: 82272662 and 22074150).

#### Conflict of interests:

The authors declared no conflict of interests.

#### REFERENCES

- Muteeb G, Rehman MT, Shahwan M, Aatif M. Origin of antibiotics and antibiotic resistance, and their impacts on drug development: A narrative review. *Pharmaceuticals* 2023;16(11):1-54.
- Helmy YA, Taha-Abdelaziz K, Hawwas HA, Ghosh S, AlKafaas SS, Moawad MM, *et al.* Antimicrobial resistance and recent alternatives to antibiotics for the control of bacterial pathogens with an emphasis on foodborne pathogens. *Antibiotics* 2023;12(2):1-52.
- Blair JM, Webber MA, Baylay AJ, Ogbolu DO, Piddock LJ. Molecular mechanisms of antibiotic resistance. *Nat Rev Microbiol* 2015;13(1):42-51.
- Darby EM, Trampari E, Siasat P, Gaya MS, Alav I, Webber MA, *et al.* Molecular mechanisms of antibiotic resistance revisited. *Nat Rev Microbiol* 2023;21(5):280-95.
- Mishra NN, Bayer AS, Tran TT, Shamoo Y, Mileykovskaya E, Dowhan W, *et al.* Daptomycin resistance in *Enterococci* is associated with distinct alterations of cell membrane phospholipid content. *PLoS One* 2012;7(8):1-10.
- Nazarov PA. MDR pumps as crossroads of resistance: Antibiotics and bacteriophages. *Antibiotics* 2022;11(6):1-18.
- Schaenzer AJ, Wright GD. Antibiotic resistance by enzymatic modification of antibiotic targets. *Trends Mol Med* 2020;26(8):768-82.
- Szychowski J, Kondo J, Zahr O, Auclair K, Westhof E, Hanessian S, *et al.* Inhibition of aminoglycoside-deactivating enzymes APH (3')-IIIa and AAC (6')-Ii by amphiphilic paromomycin O<sup>2''</sup>-ether analogues. *ChemMedChem* 2011;6(11):1961-66.

9. Ramirez MS, Tolmasky ME. Aminoglycoside modifying enzymes. *Drug Resist Updat* 2010;13(6):151-71.
10. Parisay I, Talebi M, Asadi S, Nikbakht MH. Antimicrobial efficacy of 2.5 % sodium hypochlorite, 2 % chlorhexidine, and 1.5 % hydrogen peroxide on *Enterococcus faecalis* in pulpectomy of necrotic primary teeth. *J Dent Mater Tech* 2021;10(2):94-101.
11. Afrasiabi S, Chiniforush N. An *in vitro* study on the efficacy of hydrogen peroxide mediated high-power photodynamic therapy affecting *Enterococcus faecalis* biofilm formation and dispersal. *Photodiagnosis Photodyn Ther* 2023;41:103310.
12. Li H, Zhou X, Huang Y, Liao B, Cheng L, Ren B. Reactive oxygen species in pathogen clearance: The killing mechanisms, the adaptation response, and the side effects. *Front Microbiol* 2021;11:1-9.
13. Lam PL, Wong RM, Lam KH, Hung LK, Wong MM, Yung LH, *et al.* The role of reactive oxygen species in the biological activity of antimicrobial agents: An updated mini review. *Chem Biol Interact* 2020;320:1-45.
14. Zhang E, Zhao X, Hu J, Wang R, Fu S, Qin G. Antibacterial metals and alloys for potential biomedical implants. *Bioact Mater* 2021;6(8):2569-612.
15. Godoy-Gallardo M, Eckhard U, Delgado LM, de Roo Puente YJ, Hoyos-Nogués M, Gil FJ, *et al.* Antibacterial approaches in tissue engineering using metal ions and nanoparticles: From mechanisms to applications. *Bioact Mater* 2021;6(12):4470-90.
16. da Silva BL, Caetano BL, Chiari-Andréo BG, Pietro RC, Chiavacci LA. Increased antibacterial activity of ZnO nanoparticles: Influence of size and surface modification. *Colloids Surf B Biointerfaces* 2019;177:440-7.
17. Sirelkhatim A, Mahmud S, Seeni A, Kaus NH, Ann LC, Bakhori SK, *et al.* Review on zinc oxide nanoparticles: Antibacterial activity and toxicity mechanism. *Nanomicro Lett* 2015;7:219-42.
18. Bergs C, Brück L, Rosencrantz RR, Conrads G, Elling L, Pich A. Biofunctionalized Zinc peroxide (ZnO<sub>2</sub>) nanoparticles as active oxygen sources and antibacterial agents. *RSC Adv* 2017;7(62):38998-9010.
19. Lin LS, Wang JF, Song J, Liu Y, Zhu G, Dai Y, *et al.* Cooperation of endogenous and exogenous reactive oxygen species induced by zinc peroxide nanoparticles to enhance oxidative stress-based cancer therapy. *Theranostics* 2019;9(24):380-400.
20. Morales-Mendoza JE, Paraguay-Delgado F, Moller JD, Herrera-Pérez G, Pariona N. Structure and optical properties of ZnO and ZnO<sub>2</sub> nanoparticles. *J Nano Res* 2019;56:49-62.
21. Chen W, Lu YH, Wang M, Kroner L, Paul H, Fecht HJ, *et al.* Synthesis, thermal stability and properties of ZnO<sub>2</sub> nanoparticles. *J Phys Chem C* 2009;113(4):1320-4.
22. Shen S, Mamat M, Zhang S, Cao J, Hood ZD, Figueroa-Cosme L, *et al.* Synthesis of CaO<sub>2</sub> nanocrystals and their spherical aggregates with uniform sizes for use as a biodegradable bacteriostatic agent. *Small* 2019;15(36):1-7.
23. Zhang R, Jiang G, Gao Q, Wang X, Wang Y, Xu X, *et al.* Sprayed copper peroxide nanodots for accelerating wound healing in a multidrug-resistant bacteria infected diabetic ulcer. *Nanoscale* 2021;13(37):15937-51.
24. Weiss RF. The solubility of nitrogen, oxygen and argon in water and seawater. *Deep-Sea Res Oceanogr Abstr* 1970;17(4):721-35.
25. Mendes CR, Dilarri G, Forsan CF, Sapata VD, Lopes PR, de Moraes PB, *et al.* Antibacterial action and target mechanisms of zinc oxide nanoparticles against bacterial pathogens. *Sci Rep* 2022;12(1):1-10.

---

This is an open access article distributed under the terms of the Creative Commons Attribution-NonCommercial-ShareAlike 3.0 License, which allows others to remix, tweak, and build upon the work non-commercially, as long as the author is credited and the new creations are licensed under the identical terms

This article was originally published in a special issue, "Emerging Therapeutic Interventions of Biopharmaceutical Sciences" *Indian J Pharm Sci* 2024;86(3) Spl Issue "219-225"